Dynamic Nuclear Magnetic Resonance Studies of the η^3-Triphenylcyclopropenyl Complexes $[M(\eta^3\text{-}C_3Ph_3)L]PF_6$ [M = Ni, Pd or Pt; L = $MeC(CH_2PPh_2)_3$]. Crystal Structure of the Platinum Derivative†

Carlo A. Ghilardi,[a] **Paolo Innocenti,**[a] **Stefano Midollini,**[a] **Annabella Orlandini**[a] **and Alberto Vacca**[b]

[a] *Istituto per lo Studio della Stereochimica ed Energetica dei Composti di Coordinazione, CNR, Via J. Nardi, 39–50132 Firenze, Italy*

[b] *Dipartimento di Chimica, Università di Firenze, Via Maragliano, 77–Firenze, Italy*

The dynamic behaviour of the three complexes $[M(\eta^3\text{-}C_3Ph_3)L]PF_6$ [M = Ni **1**, Pd **2** or Pt **3**; L = 1,1,1-tris(diphenylphosphinomethyl)ethane] has been investigated through $^{13}C\text{-}\{^1H\}$ variable-temperature NMR spectroscopy. The spectra indicate a temperature-dependent fluxionality of the cyclopropenyl ring, with the rotational barrier increasing in the order Ni < Pd < Pt. The molecular structure of **3**, established by single-crystal X-ray diffraction studies, shows that the co-ordination geometry of the platinum complex is fully comparable with that of the nickel analogue, indicating no correlation between structural parameters and fluxional behaviour. Crystal data for **3**: monoclinic, space group $P2_1/n$, $a = 17.129(3)$, $b = 17.517(3)$, $c = 17.968(7)$ Å, $\beta = 95.11(3)°$, $Z = 4$, $R = 0.037$.

Although the dynamic behaviour of transition-metal complexes of C_nH_n and related rings has been investigated for many years, little attention has been devoted to η^3-cyclopropenyl complexes.[1] In general the activation barrier to rotation about the C_3 axis of the C_3R_3 ligand, which has been found to vary significantly on changing the nature of the ML_n fragment, is determined by different factors, such as the oxidation state of the metal centre, the co-ordination number, and the nature of the ancillary ligands, as well as by the substituents on the C_3 ring and the interaction modes in the M–C_3 fragment. Recently the free energy of activation ($\Delta G^\ddagger$) has been measured for the cyclopropenium ring rotation in molybdenum, ruthenium, cobalt, rhodium and iridium derivatives, allowing a quantitative correlation between the electronic and steric effects of the ancillary ligands.[2]

Several years ago some of us reported the synthesis and the structural characterisation of the complex $[Ni(\eta^3\text{-}C_3Ph_3)L]BPh_4$ [L = 'triphos' = 1,1,1-tris(diphenylphosphinomethyl)ethane].[3] The shape of the resonance of the ring-carbon atoms in the $^{13}C\text{-}\{^1H\}$ NMR spectrum of this compound, at room temperature, indicated rapid rotation of the cyclopropenyl ring. Thus it seemed interesting to investigate the dynamic behaviour of $[Ni(C_3Ph_3)L]^+$ and the palladium and platinum analogue using variable-temperature $^{13}C\text{-}\{^1H\}$ NMR spectroscopy. To our knowledge this is the first case in which the dynamic behaviour of a cyclopropenium group is investigated in complexes in which the ring-carbon atoms are all chemically equivalent. For comparison the crystal structure of the platinum derivative has been determined and is also reported herein.

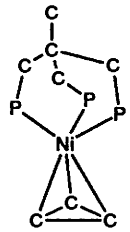

Experimental

General Procedures.—All reactions were performed under a dinitrogen atmosphere, using standard Schlenk techniques. The $^{13}C\text{-}\{^1H\}$ (50.32 MHz) and $^{31}P\text{-}\{^1H\}$ (81.015 MHz) NMR spectra were obtained on a Bruker AC-200 spectrometer. The complex $[Cr(acac)_3]$ (acac = acetylacetonate) was added to the samples used in the measurement of ^{13}C spectra. The $^{31}P\text{-}\{^1H\}$ chemical shifts were recorded in ppm and referenced to external 85% H_3PO_4, the $^{13}C\text{-}\{^1H\}$ chemical shifts in ppm downfield from $SiMe_4$ and referenced to internal dichlorodideuteriomethane.

Starting Materials.—The complexes $[M(C_2H_4)(PPh_3)_2]$, (M = Ni,[4] Pd[5] or Pt[6]) and the cyclopropenyl salt $[C_3Ph_3]PF_6$[7] were prepared as previously described.

Preparation of Complexes.—$[Ni(C_3Ph_3)L]PF_6$ **1**. The complex was prepared using a method analogous to that previously described for the tetraphenylborate salt.[3] Solid $[C_3Ph_3]PF_6$ (412 mg, 1 mmol) was added, at room temperature with continuous stirring, to a solution of $[Ni(C_2H_4)(PPh_3)_2]$ (611 mg, 1 mmol) in tetrahydrofuran (thf) (30 cm^3). Solid L (625 mg, 1 mmol) was then added. After 30 min, butanol (20 cm^3) was added and the solvent was evaporated in a flow of nitrogen. Red-orange crystals precipitated; these were filtered off, washed with butanol, and recrystallised from dichloromethane–butanol. Yield: 960 mg, 88% (Found: C, 68.05; H, 5.10; Ni, 5.30. Calc. for $C_{62}H_{54}F_6NiP_4$: C, 67.95; H, 4.95; Ni, 5.35%). Selected NMR data (CD_2Cl_2, 298 K): $^{13}C\text{-}\{^1H\}$, δ 63.2 (q, $^2J_{PC} = 6$, C_{ring}), 38.90 (q, $^3J_{PC} = 10$, CH_3), 35.80 (q, $^2J_{PC} = 3$ Hz, CCH_3) and 34.7 (m, CH_2).

$[Pd(C_3Ph_3)L]PF_6$ **2**. This complex was prepared similarly

---

† *Supplementary data available:* see Instructions for Authors, *J. Chem. Soc., Dalton Trans.*, 1995, Issue 1, pp. xxv–xxx.

using $[Pd(C_2H_4)(PPh_3)_2]$ as the starting material. Orange crystals, yield 92% (Found: C, 65.05; H, 4.85; Pd, 9.15. Calc. for $C_{62}H_{54}F_6P_4Pd$: C, 65.20; H, 4.75; Pd, 9.30%). Selected NMR data (CD_2Cl_2, 298 K): $^{31}P\text{-}\{^1H\}$, δ −7.5; $^{13}C\text{-}\{^1H\}$, δ 67.7 (q, $^2J_{PC}$ = 7, C_{ring}), 40.1 (q, $^3J_{PC}$ = 11, CH_3), 35.3 (m, CH_2) and 32.9 (q, $^2J_{PC}$ = 4 Hz, CCH_3).

$[Pt(C_3Ph_3)L]PF_6$ **3**. The complex was prepared similarly using $[Pt(C_2H_4)(PPh_3)_2]$ as the starting material. Yellow crystals, yield 89% (Found: C, 60.30; H, 4.50; Pt, 15.70. Calc. for $C_{62}H_{54}F_6P_4Pt$: C, 60.45; H, 4.40; Pt, 15.85%). Selected NMR data (CD_2Cl_2, 298 K): $^{31}P\text{-}\{^1H\}$, δ 26.25 (s with satellites, $^1J_{PtP}$ = 2682 Hz); $^{13}C\text{-}\{^1H\}$, δ 40.3 (q, $^3J_{PC}$ = 11, CH_3), 39.7 (q with satellites, $^2J_{PC}$ = 2, $^4J_{PtC}$ = 30, CCH_3), 36.5–36.4 (m with satellites, $^1J_{PtC}$ = 162 Hz, C_{ring}) and 34.7–33.7 (m, CH_2).

Single-crystal Structure Determination.—Diffraction data for complex **3** were collected at room temperature on an Enraf-Nonius CAD4 automatic diffractometer. Unit-cell parameters were determined by least-squares refinement of the setting angles of 25 carefully centred reflections. Crystal and data collection details are given in Table 1. The intensities I as well as the standard deviations $\sigma(I)$ were calculated as described elsewhere, by using the value of 0.03 for the instability factor k.[8] After rescaling, the intensities were corrected for Lorentz-polarisation and for absorption effects.[9]

All the calculations were carried out on an HP 486/25 personal computer, using the SHELX 76[10] and PLUTO[11] programs. Atomic scattering factors for non-hydrogen atoms were taken from ref. 12 and those for hydrogen from ref. 13. Both $\Delta f'$ and $\Delta f''$ components of the anomalous dispersion were included for all non-hydrogen atoms.[14] Patterson and Fourier maps enabled the location of all the atoms. Full-matrix least-squares refinements were carried out with anisotropic thermal parameters assigned to platinum, phosphorus and fluorine atoms. The phenyl rings were treated as rigid bodies of D_{6h} symmetry. During the refinement the function $\Sigma w(|F_o| - |F_c|)^2$ was minimised, the weights, w, being defined as $1/\sigma^2(F_o)$. Refinement converged to $R = R' = 0.037$. Table 2 reports the final positional parameters.

Additional material available from the Cambridge Crystallographic Data Centre comprises H-atom coordinates, thermal parameters and remaining bond distances and angles.

Computer Analysis of the NMR Spectra.—The NMR spectra were simulated using a locally developed computer package containing the programs LAOCN,[15] DAVINS[16] and DNMR,[17] adapted for a personal computer.

The digitised spectra, consisting of a sequence of intensity values of spectral points equally spaced in frequency, were transferred from the spectrometer computer by means of the Bruker WIN-NMR computer package.[18] The line shape-fitting least-squares analysis was performed by searching the set of parameters (chemical shifts, coupling constants, rate constants, transverse relaxation times T_2, *etc.*) which gave the minimum sum of the squared residuals between experimental and calculated intensities at each spectral point. Since the intensity scale of the NMR spectra was arbitrary, the residuals were scaled by dividing them by the intensity of the highest peak in the corresponding spectral window. The root-mean-square scaled residual, expressed in percent, was used as agreement factor. The error-square sum was minimised according to the conjugated-directions method of Powell.[19]

Results and Discussion

Structure of Complex **3**.—The molecular structure of complex **3** consists of $[Pt(C_3Ph_3)L]^+$ cations and hexafluorophosphate anions. Fig. 1 shows a perspective view of the complex cation. Table 3 reports selected bond distances and angles.

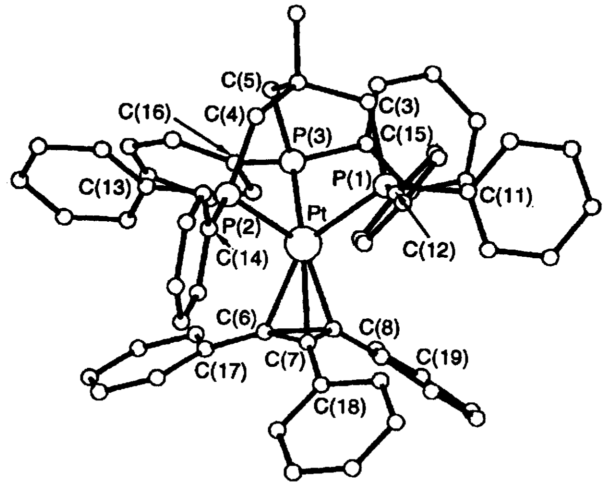

Fig. 1 Perspective view of the complex cation $[Pt(\eta^3\text{-}C_3Ph_3)L]^+$ (PLUTO drawing)

Table 1 Crystal data and data collection details for complex **3**

Formula	$C_{62}H_{54}F_6P_4Pt$
M	1232.1
Crystal symmetry	Monoclinic
Space group	$P2_1/n$
a/Å	17.129(3)
b/Å	17.517(3)
c/Å	17.968(7)
β/°	95.11(3)
U/Å^3	5369.8
Z	4
D_c/g cm^{-3}	1.524
F(000)	2472
Habit	Parallelepiped
Dimensions/mm	0.25 × 0.25 × 0.40
μ/cm^{-1}	28.1
Absorption correction range	0.91–1.15
Radiation	Mo-Kα, λ = 0.7107 Å
Monochromator	Graphite crystal
Method	ω–2θ
Scan speed (°min^{-1})	8.24
Scan width/°	0.7 + 0.35 tan θ
Background time	Half the scan time
Standards	3 every 120 min
Maximum deviation (%)	2
2θ limits/°	5–45
Number of data [$I > 3\sigma(I)$]	5486
Final number of variables	246

In the complex cation the platinum centre is linked to the three phosphorus atoms of the ligand L and to the cyclopropenyl fragment in a symmetric η^3 fashion; the orientation of the cyclopropenyl ring is staggered with respect to L. The values of the bond distances and angles within the PtL fragment are well within the range reported in the literature; in fact the P–Pt–P angles [87.4(1), 89.2(1) and 89.8(1)°] match the values in a variety of transition-metal complexes of L.[20] The Pt–P bond distances [2.359(2), 2.381(2) and 2.381(2) Å], with the shortest value opposite the smallest P–Pt–P angle, appear normal (sum of covalent radii 2.36 Å).

Concerning the linkage Pt–C_3Ph_3, the range of Pt–C distances, 2.131(7)–2.167(7) Å, is small, and the slight differences seem insignificant. The average value (2.149 Å), taking into account the different covalent radii (Pt 1.30 and Ni 1.15 Å), agrees well with the corresponding value found in the analogous $[Ni(C_3Ph_3)L]^+$ cation (2.03 Å).[3] The platinum centre lies 1.979 Å from the C_3 ring, which is very regular, with the inner C–C distances practically identical [range 1.445(9)–1.448(10) Å], as are the exocyclic C–C bonds [range 1.453(8)–1.478(9) Å]. It is noteworthy that the large values of the 'tilt'

Table 2 Final atomic coordinates ($\times 10^4$; except Pt, $\times 10^5$)

Atom	*x*	*y*	*z*
Pt	5 456(2)	20 931(2)	29 375(2)
P(1)	284(1)	2 965(1)	1 929(1)
P(2)	1 681(1)	1 676(1)	2 405(1)
P(3)	1 297(1)	3 079(1)	3 568(1)
C(1)	2 545(5)	3 799(5)	1 814(5)
C(2)	1 947(4)	3 288(4)	2 155(4)
C(3)	1 135(4)	3 600(4)	1 876(4)
C(4)	2 075(4)	2 461(4)	1 876(4)
C(5)	2 106(4)	3 351(5)	3 017(4)
C(6)	163(4)	1 219(4)	3 678(4)
C(7)	−299(4)	1 189(4)	2 965(4)
C(8)	−449(4)	1 777(4)	3 501(4)
C(11)	−538(3)	3 628(3)	1 921(3)
C(21)	−1 214(3)	3 367(3)	2 218(3)
C(31)	−1 859(3)	3 851(3)	2 241(3)
C(41)	−1 826(3)	4 595(3)	1 969(3)
C(51)	−1 150(3)	4 855(3)	1 672(3)
C(61)	−505(3)	4 372(3)	1 648(3)
C(12)	164(4)	2 561(2)	989(3)
C(22)	155(4)	3 032(2)	362(3)
C(32)	114(4)	2 711(2)	−351(3)
C(42)	82(4)	1 920(2)	−437(3)
C(52)	91(4)	1 449(2)	191(3)
C(62)	132(4)	1 770(2)	904(3)
C(13)	2 492(2)	1 309(3)	3 040(3)
C(23)	2 363(2)	1 130(3)	3 776(3)
C(33)	2 963(2)	807(3)	4 250(3)
C(43)	3 691(2)	661(3)	3 988(3)
C(53)	3 819(2)	839(3)	3 252(3)
C(63)	3 220(2)	1 163(3)	2 779(3)
C(14)	1 610(3)	887(3)	1 744(2)
C(24)	1 184(3)	249(3)	1 934(2)
C(34)	1 125(3)	−385(3)	1 463(2)
C(44)	1 493(3)	−380(3)	800(2)
C(54)	1 919(3)	258(3)	610(2)
C(64)	1 977(3)	892(3)	1 081(2)
C(15)	743(3)	3 956(3)	3 684(3)
C(25)	−64(3)	3 901(3)	3 727(3)
C(35)	−500(3)	4 554(3)	3 851(3)
C(45)	−130(3)	5 262(3)	3 931(3)
C(55)	678(3)	5 317(3)	3 888(3)
C(65)	1 114(3)	4 664(3)	3 765(3)
C(16)	1 793(3)	2 960(3)	4 510(3)
C(26)	2 559(3)	2 688(3)	4 636(3)
C(36)	2 884(3)	2 555(3)	5 365(3)
C(46)	2 443(3)	2 695(3)	5 967(3)
C(56)	1 677(3)	2 967(3)	5 841(3)
C(66)	1 352(3)	3 100(3)	5 112(3)
C(17)	560(3)	790(3)	4 292(2)
C(27)	787(3)	35(3)	4 189(2)
C(37)	1 192(3)	−363(3)	4 775(2)
C(47)	1 372(3)	−6(3)	5 462(2)
C(57)	1 146(3)	749(3)	5 565(2)
C(67)	740(3)	1 147(3)	4 980(2)
C(18)	−748(3)	673(2)	2 449(2)
C(28)	−712(3)	−117(2)	2 546(2)
C(38)	−1 177(3)	−593(2)	2 068(2)
C(48)	−1 679(3)	−279(2)	1 494(2)
C(58)	−1 715(3)	510(2)	1 397(2)
C(68)	−1 250(3)	987(2)	1 875(2)
C(19)	−1 144(3)	2 077(3)	3 835(3)
C(29)	−1 883(3)	2 019(3)	3 443(3)
C(39)	−2 542(3)	2 292(3)	3 760(3)
C(49)	−2 464(3)	2 623(3)	4 469(3)
C(59)	−1 726(3)	2 682(3)	4 861(3)
C(69)	−1 066(3)	2 408(3)	4 544(3)
P(4)	4 836(2)	2 611(2)	1 994(2)
F(1)	3 968(4)	2 375(5)	1 720(5)
F(2)	5 015(5)	1 775(4)	2 228(5)
F(3)	5 731(5)	2 806(5)	2 145(6)
F(4)	5 038(5)	2 314(7)	1 181(4)
F(5)	4 641(6)	3 410(5)	1 716(8)
F(6)	4 607(8)	2 824(8)	2 738(5)

Table 3 Selected bond distances (Å) and angles (°)

Pt–P(1)	2.381(2)	P(2)–C(14)	1.820(5)
Pt–P(2)	2.359(2)	P(3)–C(5)	1.837(8)
Pt–P(3)	2.381(2)	P(3)–C(15)	1.827(5)
Pt–C(6)	2.167(7)	P(3)–C(16)	1.837(5)
Pt–C(7)	2.148(7)	C(6)–C(7)	1.445(9)
Pt–C(8)	2.131(7)	C(6)–C(8)	1.446(10)
P(1)–C(3)	1.843(8)	C(6)–C(17)	1.453(8)
P(1)–C(11)	1.824(6)	C(7)–C(8)	1.448(10)
P(1)–C(12)	1.825(6)	C(7)–C(18)	1.463(8)
P(2)–C(4)	1.833(8)	C(8)–C(19)	1.478(9)
P(2)–C(13)	1.834(5)		
P(1)–Pt–P(2)	89.77(6)	P(3)–Pt–C(6)	113.6(2)
P(1)–Pt–P(3)	87.38(7)	P(3)–Pt–C(7)	149.4(2)
P(2)–Pt–P(3)	89.24(7)	P(3)–Pt–C(8)	112.6(2)
P(1)–Pt–C(6)	150.8(2)	C(7)–C(6)–C(8)	60.1(5)
P(1)–Pt–C(7)	114.1(2)	C(6)–C(7)–C(8)	60.0(5)
P(1)–Pt–C(8)	115.1(2)	C(6)–C(8)–C(7)	59.9(5)
P(2)–Pt–C(6)	109.6(2)	Pt–C(6)–C(17)	133.2(5)
P(2)–Pt–C(7)	111.2(2)	Pt–C(7)–C(18)	139.3(5)
P(2)–Pt–C(8)	146.6(2)	Pt–C(8)–C(19)	143.9(5)

angles (19.2–32.2°) are even larger than in the nickel analogue (20.1–30.3°). The 'twist' angles, defined as in ref. 21, display values ranging from 12.8 to 31.9°. Such enhancement of the bending of the C_3Ph_3 phenyl groups in both compounds of L with respect to the free cyclopropenium cation[22] and other M–C_3 complexes[21,23] is likely due to the steric repulsion exerted by the bulky ligand L on the phenyl rings of the cyclopropenyl fragment.

Taking into account the different covalent radii, the nickel and platinum complexes do not seem to display structural features which can be correlated with their dynamic behavioural differences.

It seems of interest to recall that a cyclopropenium platinum derivative with only two phosphine ligands, namely $[Pt(C_3Ph_3)(PPh_3)_2]$,[24] displays a completely different C_3Ph_3 bonding mode, containing a localised cyclopropenyl ring with an asymmetrical η^2 linkage. Within the series $[MC_3L_2]X$ (M = Ni, Pd or Pt) the ring-whizzing motion, *i.e.* a type of fluxionality where the ML_2 unit migrates over the face of the cyclopropenium cation, has been ascertained and discussed exhaustively.[25]

NMR Studies.—The room-temperature $^{31}P-\{^1H\}$ NMR spectra of the complexes (see Experimental section) consist of a singlet (with platinum satellites in the case of **3**), demonstrating the equivalence of the three co-ordinated phosphorus atoms. The room-temperature spectrum of a solution containing equimolar amounts of **2** and free L indicated that there was no exchange between co-ordinated and free L on the NMR time-scale. An intramolecular rearrangement in which the phosphorus positions are permuted without bond breaking appears quite unlikely in the present cases owing to the rigidity of the chelate ligand L.

The cyclopropenyl ring-carbon nuclei in these complexes are magnetically equivalent and a single resonance is observed in their $^{13}C-\{^1H\}$ NMR spectra. Owing to the coupling with the three phosphorus nuclei of the ligand L, different profiles for the signal are expected for a rigid or a fluxional structure, respectively, the quartet line shape being consistent with a rapidly rotating C_3Ph_3 group on the NMR time-scale. The ^{13}C-

{^{1}H} spectra of **1**–**3**, at room temperature, exhibited, as expected, different types of resonances: the ^{13}C$_{ring}$ resonances of **2** appear as quartets, while the corresponding signal of **3** consisted of a doublet of broad multiplets. Moreover, both compounds exhibit a temperature-dependent fluxional behaviour: the ^{13}C-{^{1}H} NMR variable-temperature spectra of **2** (range 203–298 K) and **3** (238–309 K) are shown in Figs. 2 and 3, respectively. The ^{13}C-{^{1}H} spectrum of **1** shows a quartet attributable to the C_3 ring atoms even at 223 K; as the temperature is further decreased the signal begins to broaden, but the poor quality of the field homogeneity in the low-temperature experiments prevented the recording of reliable spectra. The solutions used in such measurements were quite concentrated.

The variable-temperature ^{13}C-{^{1}H} NMR spectra of complex **2** are well suited to a dynamic NMR analysis, as the explored temperature range covers the conditions for both slow and fast exchange. The dynamic process can be satisfactorily described in terms of a mutual exchange equilibrium between the staggered structures outlined in Scheme 1, which affords an AXX'$_2$ spin system, where A = ^{13}C and X = ^{31}P, and a fluxional structure (an AX$_3$ spin system). A computer fitting of all of the measured spectra of **2**, as described in the Experimental section, was performed using as parameters (*i*) the chemical shifts of the ^{13}C nucleus, δ_A (one at each temperature), (*ii*) the coupling constants J_{AX}, $J_{AX'}$ and $J_{XX'}$, assumed to be temperature independent, (*iii*) the relaxation time T_2, and (*iv*) the rate constants k (one at each temperature). The minimisation procedure converged to an agreement factor of 5.06%: the results are listed in Table 4 and the simulated spectra are shown in Fig. 2.

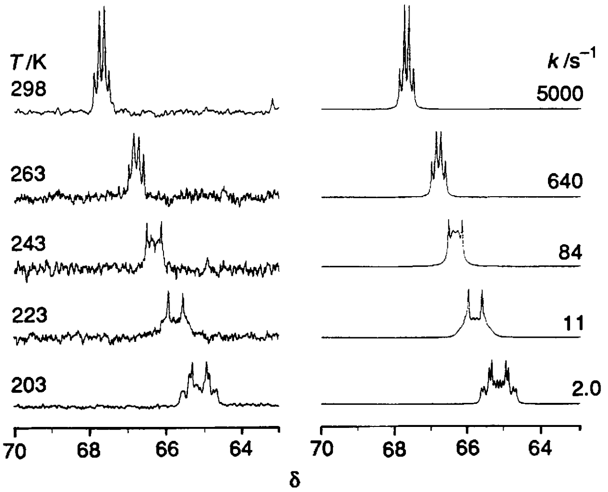

Fig. 2 Observed (left) and simulated (right) variable-temperature ^{13}C-{^{1}H} NMR spectra of complex **2**

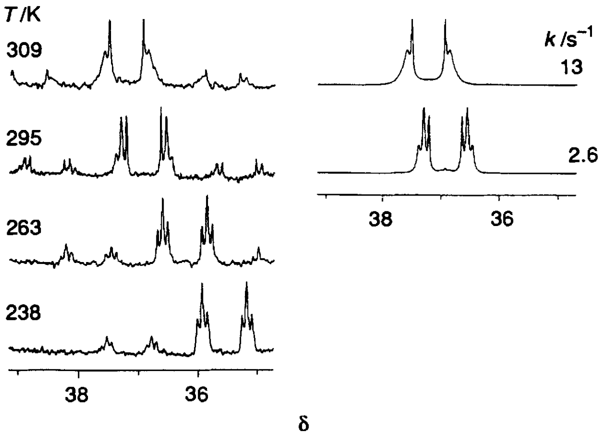

Fig. 3 Observed (left) and simulated (right) variable-temperature ^{13}C-{^{1}H} NMR spectra of complex **3**

Plotting ln k *vs.* T^{-1} results in an interpolated least-squares straight line (linear correlation coefficient $r = 0.997$), from which the activation parameters $E_a = 43 \pm 2$ kJ mol^{-1}, $\Delta H^‡ = 40 \pm 2$ kJ mol^{-1}, and $\Delta S^‡ = -38 \pm 9$ J K^{-1} mol^{-1} can be obtained (Fig. 4). At room temperature, a $\Delta G^‡$ (298 K) value of 52 ± 4 kJ mol^{-1} was calculated. This value of the free energy of activation is comparable with corresponding values reported for other non-rigid η^3-cyclopropenyl complexes of transition metals,[2d,e] which are spread over the range 40–80 kJ mol^{-1}.* To our knowledge this is the first time that values of $\Delta H^‡$ and $\Delta S^‡$ for cyclopropenyl rotation in metal complexes have been determined. The negative value of the entropy of activation, consistent with a non-dissociative mechanism, may be ascribed to the decrease in the number of accessible energy states in the activated complex with respect to the stable staggered conformation. In the absence of literature values of $\Delta S^‡$, a reasonable comparison may be to η^4-trimethylenemethane complexes, in which the three-fold nature of the ligand rotation is closest to that present in our compound. The values of $\Delta S^‡$ reported for seven trimethylenemethane iron complexes are negative, with only one exception, ranging from 2 to −80 J K^{-1} mol^{-1}.[26]

Unfortunately, an analogous determination of the activation parameters could not be performed from the ^{13}C NMR spectra of the nickel and platinum complexes. The fluxional process appears to afford barely significant changes in the experimental resonances and only in the lower and upper bounds of the

Table 4 Refined parameters from least-squares minimisation of the variable-temperature ^{13}C NMR spectra of complex **2**

T/K	δ_A	k/s^{-1}
203	65.14	2.0
223	65.76	11
243	66.32	84
263	66.80	6.4×10^2
298	67.70	5.0×10^3

$J_{AX} = 26.7$, $J_{AX'} = -3.7$, $J_{XX'} = -10.6$ Hz; $T_2 = 0.13$ s.

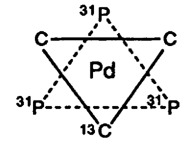

Scheme 1

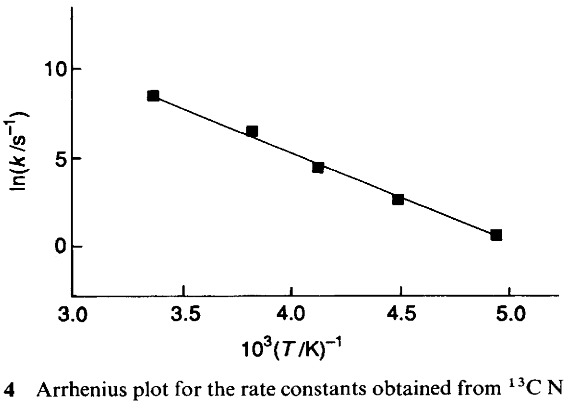

Fig. 4 Arrhenius plot for the rate constants obtained from ^{13}C NMR data of complex **2**

---

* The barriers to ring rotation in the hypothetical [Fe(η^3-C$_3$H$_3$)(CO)$_3$]$^-$ and [Co(η^3-C$_3$H$_3$)(CO)$_3$] complexes have been calculated by extended-Hückel molecular-orbital methods to be about 28 kJ mol^{-1}.[1b,c]

exploitable temperature range for **1** and **3**, respectively. In any case, by assuming that the same exchange mechanism $\mathrm{AXX'_2 \rightleftharpoons AX_3}$ is involved, a dynamic NMR optimisation of the ^{13}C NMR spectra of the platinum derivative **3** at 295 and 309 K converges to a minimum (with an agreement factor of 3.96%) (Fig. 3), giving the following parameters: $\delta_A = 36.95$ and 37.25 (at 295 and 309 K, respectively), $J_{AX} = 37.0$, $J_{AX'} = -4.2$ and $J_{XX'} = -3.6$ Hz, $t_2 = 0.20$ s, and $k = 2.6$ and 13 s^{-1} (at 295 and 309 K, respectively). By inserting the k value measured at 295 K into the Eyring equation,[27] one obtains a free energy of activation, $\Delta G^{\ddagger}$ (295 K), of 71 kJ mol^{-1}, which is much larger than the corresponding value determined for the palladium compound. A very rough evaluation of the rate constant from the line-shape fitting of the ^{13}C NMR spectrum of the nickel derivative at 223 K affords a value of about 10^3 s^{-1}. Substituting this value into the Eyring equation, one obtains a $\Delta G^{\ddagger}$ value (at 223 K) of about 40 kJ mol^{-1}. This is, as expected, considerably lower than the values for the other two compounds, even when taking into account that they refer to different temperatures.

Comparison of the $\Delta G^{\ddagger}$ values obtained for the complexes **1**–**3** demonstrates that the rotational barrier of the cyclopropenyl fragment grows significantly on descending the group. This finding is in agreement with the trend already observed by Hughes *et al.*[2e] for the η^3-cyclopropenyl complexes of Co, Rh and Ir, and with the general observation made for rotational barriers of olefin and 1,3-diene complexes of transition metals.[1a]

Acknowledgements

Thanks are due to Mr. F. Cecconi and Mr. G. Scapacci for technical assistance and to Mr. F. Nuzzi for microanalyses.

References

1 (*a*) B. L. Mann, in *Comprehensive Organometallic Chemistry*, eds. G. Wilkinson, E. Abel and F. G. A. Stone, Pergamon, Oxford, 1983, vol. 3, ch. 20, p. 89; (*b*) T. A. Albright, P. Hoffmann and R. Hoffmann, *J. Am. Chem. Soc.*, 1977, **99**, 7546; (*c*) T. A. Albright, *Acc. Chem. Res.*, 1982, **15**, 149.

2 (*a*) M. R. Churchill, J. C. Fettinger, L. G. McCullough and R. R. Schrock, *J. Am. Chem. Soc.*, 1984, **106**, 3356; (*b*) R. P. Hughes, J. Robbins, D. J. Robinson and A. L. Rheingold, *J. Am. Chem. Soc.*, 1988, **7**, 2413; (*c*) D. L. Lichtenberger, M. L. Hoppe, L. Subramanian, E. M. Kober, R. P. Hughes, J. L. Hubbard and D. S. Tucker, *Organometallics*, 1993, **12**, 2025; (*d*) R. Ditchfield, R. P. Hughes, D. S. Tucker, E. P. Bierwagen, J. Robbins, D. J. Robinson and J. A. Zakutansky, *Organometallics*, 1993, **12**, 2258; (*e*) R. P. Hughes, D. S. Tucker and A. L. Rheingold, *Organometallics*, 1993, **12**, 3069, (*f*) R. P. Hughes and D. S. Tucker, *Organometallics*, 1993, **12**, 4736.

3 C. Mealli, S. Midollini, S. Moneti and L. Sacconi, *J. Organomet. Chem.*, 1981, **205**, 273.

4 P. Giannoccaro, A. Sacco and G. Vasapollo, *Inorg. Chim. Acta*, 1979, **37**, L455.

5 A. Visser, R. Van der Linde and R. O. De Young, *Inorg. Synth.*, 1976, **16**, 127.

6 O. J. Sherer and H. Jungmann, *J. Organomet. Chem.*, 1981, **208**, 153.

7 R. Breslow and H. W. Chang, *J. Am. Chem. Soc.*, 1961, **83**, 2374.

8 P. W. R. Corfield, R. J. Doedens and J. A. Ibers, *Inorg. Chem.*, 1967, **6**, 197.

9 N. Walker and D. Stewart, *Acta Crystallogr., Sect. A*, 1983, **39**, 158.

10 G. M. Sheldrick, SHELX 76, System of Computing Programs, University of Cambridge, 1976.

11 PLUTO, Cambridge Crystallographic Data Centre, University Chemical Laboratory, Cambridge, 1989.

12 *International Tables for X-Ray Crystallography*, Kynoch Press, Birmingham, 1974, vol. 4, p. 99.

13 R. F. Stewart, E. R. Davidson and W. T. Simpson, *J. Chem. Phys.*, 1965, **42**, 3175.

14 *International Tables for X-Ray Crystallography*, Kynoch Press, Birmingham, 1974, vol. 4, p. 149.

15 S. Castellano and A. A. Bothner-By, *J. Chem. Phys.*, 1964, **41**, 3863.

16 D. S. Stephenson and G. Binsch, *J. Magn. Reson.*, 1980, **37**, 395.

17 D. A. Klier and G. A. Binsch, *J. Magn. Reson.*, 1970, **3**, 146.

18 H. Thiele, *WIN-NMR Manual*, Bruker Spectrospin, Fällanden, 1991.

19 M. J. D. Powell, *Comput. J.*, 1964, **7**, 155; W. H. Press, B. P. Flannery, S. A. Teukolsky and W. T. Vetterling, in *Numerical Recipes* (*FORTRAN Version*), Cambridge University Press, 1989, p. 294.

20 P. Zanello, A. Cinquantini, C. A. Ghilardi, S. Midollini, S. Moneti, A. Orlandini and A. Bencini, *J. Chem. Soc., Dalton Trans.*, 1990, 3761; C. A. Ghilardi, C. Mealli, V. Nefedov, A. Orlandini and L. Sacconi, *Inorg. Chem.*, 1980, **19**, 2454.

21 R. M. Tuggle and D. L. Weaver, *Inorg. Chem.*, 1971, **10**, 1504.

22 M. Sundaralingam and L. H. Jensen, *J. Am. Chem. Soc.*, 1966, **88**, 198.

23 R. M. Tuggle and D. L. Weaver, *Inorg. Chem.*, 1971, **10**, 2599; T. Chiang, R. C. Kerber, S. D. Kimball and J. W. Lauher, *Inorg. Chem.*, 1979, **18**, 1687.

24 M. D. McClure and D. L. Weaver, *J. Organomet. Chem.*, 1973, **54**, C59.

25 C. Mealli, S. Midollini, S. Moneti, L. Sacconi, J. Silvestre and T. A. Albright, *J. Am. Chem. Soc.*, 1982, **104**, 95.

26 L. Girard and M. C. Baird, *J. Organomet. Chem.*, 1993, **444**, 143.

27 H. Eyring, *Chem. Rev.*, 1935, **17**, 65.

Received 29*th September* 1994; *Paper* 4/05979D